Thermal hysteresis and phase front shape at para-ferro transition in DKDP crystals under small dc applied electric fields

2000 J. Phys.: Condens. Matter 12 7819

(http://iopscience.iop.org/0953-8984/12/35/316)

J. Phys.: Condens. Matter **12** (2000) 7819–7831. Printed in the UK PII: S0953-8984(00)13732-4

Thermal hysteresis and phase front shape at para–ferro transition in DKDP crystals under small dc applied electric fields

Zdének Kvitek† and Jean Bornarel‡

† Zkusebnictvi a.s.—High Power Laboratory, 19011 Praha 9, Bechovice, Czech Republic
‡ Laboratoire de Spectrométrie Physique (UMR 5588), Université Joseph Fourier (Grenoble I), Boite postale No 87, 38402 Saint-Martin-d'Hères Cédex, France

Received 4 May 2000, in final form 13 July 2000

Abstract. Observation of the phase front and the domains during the paraelectric–ferroelectric KD_2PO_4 phase transition has been performed under small dc applied electric fields E_z. The dielectric ε_c' and loss ε_c'' constants have been simultaneously measured. A special phenomenon during heating cycles is observed with creation of a heterophase region with alternating paraelectric and polydomain ferroelectric stripes in a sample which is essentially monodomain. This is explained with the help of the mechanical energy calculation due to the inclusion.

The increasing of the thermal hysteresis at the transition when a small dc electric field (or stress) is applied to the crystal is also explained.

1. Introduction

The KD_2PO_4 (DKDP) crystal undergoes a first-order transition between a tetragonal paraelectric and paraelastic phase ($\bar{4}2m$) which is the high-temperature phase, and an orthorhombic ferroelectric and ferroelastic one ($mm2$). The polarization that is considered as the order parameter belongs to the B_2 representation as does the shear strain u_{xy} due to the piezoelectric behaviour of DKDP. Besides the shear strain appearance in the plane perpendicular to the ferroelectric axis c, it is possible to notice values of normal lattice deformation with $u_{zz} = 6.5 \times 10^{-4}$ greater than u_{xx} and u_{yy} (about 1×10^{-4}). In the low-temperature phase the ferroelectric–ferroelastic domain structure exists with permissible walls (Fousek and Janovec 1969) in (100) and (010) tetragonal planes. These domains are also mechanical twins (Bornarel and Lajzerowicz 1968).

The character of the DKDP phase transition was always observed to be a first order one. However the existence of a thermal hysteresis at the transition has been clarified only recently. Then the possible theoretical range for the thermal hysteresis ΔT calculated with the help of Landau–Devonshire theory is about 0.2 K (Sidnenko and Gladkii 1973, Chabin and Gilletta 1977) and some authors observed thermal hysteresis equal to a few tenths of a degree. But other studies in DKDP crystals have also proved that the phase transition can occur without thermal hysteresis (Reese and May 1968, Zeyen *et al* 1976, Reese 1969). The situation has been recently clarified by simultaneous optical observations and dielectric measurements (Bornarel and Cach 1999): DKDP crystals without applied electric field or mechanical stress, in thermal gradient equal to or lower than 5×10^{-3} K mm^{-1}, undergo phase coexistence without thermal hysteresis (with an accuracy equal to 10^{-2} K). This result is important for the present paper.

0953-8984/00/357819+13$30.00

In the last ten years the phase coexistence of DKDP has been systematically studied in crystals without applied electric field or mechanical stress. The great importance of an external thermal gradient $\vec{G}_e$ to the coexistence phenomena and the phase front shape has been demonstrated when $\vec{G}_e$ is greater than 10^{-2} K mm^{-1}. When $\vec{G}_e$ is parallel to the ferroelectric c axis, the phase front is quasiplanar and near the (001) plane (Bornarel and Cach 1993). When $\vec{G}_e$ is perpendicular to the c axis, the phase front appears like a factory roof the section of which in the a_1 (or a_2) tetragonal plane has a zig-zag shape (Bornarel and Cach 1991, Bornarel *et al* 1996). The phase front makes an angle lower than 25° with the (001) plane. When the thermal gradient is small enough, for example 5×10^{-3} K mm^{-1}, only one or two quasiplanar phase fronts near the (001) plane take part in the phase coexistence (Kvitek and Bornarel 1997, Bornarel and Cach 1999). A theoretical model explains these phenomena as a competition between the mechanical and chemical energies, with a quasi-negligible effect of the electrostatic energy at zero applied electric field (Kvitek 1997).

Optical observations of the domain texture (and of the phase front) performed simultaneously with dielectric measurements allowed us to demonstrate that the dielectric constant ε'_c can be considered as the sum of three contributions: the contribution of a monodomain sample, the contribution of the domains and the contribution due to the phase front existence during the phase coexistence (Bornarel and Cach 1999). These previous results have been obtained without applied electric field. In the present paper, a phase coexistence in crystals under a small external applied electric field and very small thermal gradient is described. The experimental procedures are given in section 2. The results on particular phase front shapes and thermal hysteresis values are described in section 3 and discussed in the last section. Khachaturyan theory is used to calculate the mechanical energy induced by the paraelectric–ferroelectric interface (Khachaturyan 1983). Then an explanation of the thermal hysteresis phenomena previously observed is proposed.

2. Experimental procedures

The DKDP crystals were grown by slow cooling of a supersaturated solution of KDP and heavy water. The observed transition at 208.7 ± 0.1 K corresponds to a deuterion concentration of about 70%. The orientations of the sample faces were verified with x-ray Bragg diffraction (accuracy of a minute of arc). The sample dimensions were $a_1 = 2.41$ mm, $a_2 = 4.71$ mm, $c = 9.02$ mm. Semitransparent gold electrodes were evaporated on the c faces.

The cryostat employed with a helium-gas exchange chamber allows optical observations and measurements along three perpendicular axes simultaneously with dielectric measurements. In the present case these three axes correspond to the tetragonal axes on the crystal. The c ferroelectric axis corresponded to a horizontal optical axis and was perpendicular to the thermal gradient $\vec{G}_e$. The thermal gradient $\vec{G}_e$ in the helium gas chamber was controlled with an accuracy of 5 mK mm^{-1} with the help of two platinum resistors placed just above and below the sample. The temperature reported further on is that of the lower platinum resistor which was measured with a precision of 2×10^{-3} K. The dielectric measurements and optical observations of the phase front were carried out under cooling and heating rates lower than 10^{-3} K min^{-1}. Each thermal cycle was performed as follows: the temperature was stabilized for several hours one degree above the temperature of transition. The sample was cooled regularly during the paraelectric–ferroelectric (PF) cycles to one degree under the transition temperature. Then the temperature is decreased and the sample is kept for 12 hours at a temperature 15 degrees under the transition temperature which simplifies and stabilizes the domain structure. Finally the temperature is increased during the ferroelastic–paraelectric (FP) cycles with the same rate in the phase coexistence temperature range.

Two thin copper wires were glued with a spot of silver paste on the faces perpendicular to the c ferroelectric axis allowing the electrical contacts for dielectric measurements and dc electric field application. The sample capacity and dissipation factor were measured using an HP 4274 A impedance meter with a measuring field of 1 V cm^{-1} in amplitude and 4 kHz in frequency allowing us to calculate ε_c' and ε_c'' with a relative accuracy of 3×10^{-3} and 1×10^{-2}, respectively. A dc electric field can also be applied simultaneously. The observations along the a_1 and a_2 axes allow us to rebuild the phase front shape while the observation along the c axis gives information on the domain texture. The diffraction of a laser beam propagating in the c direction has also been used to detect the presence of the domains (Hill and Ichiki 1964).

3. Results

The results obtained simultaneously concerning the phase front shape, the domain structure and the dielectric ε_c' and loss ε_c'' constants are presented successively to make them clearer.

3.1. Phase front and domain structure

In the experimental conditions previously described, the evolution of the phase front is similar during PF and FP cycles when dc applied electric field E_z is lower than 250 V cm^{-1}. At the beginning of a PF transition, the phase front appears at the same time in all sample corners (Bornarel and Cach 1999) or in the coldest sample corners. The tetragonal phase grows very quickly in the $\vec{G}_e$ direction (a_1 direction in figure 1) so that the phase front adopts a quasiplanar shape slightly sloped to the (001) plane. Sometimes before a phase front sweeps the whole sample away in the c direction, a new planar phase front is created on the opposite c face towards the former. The β angle between the phase front and the (001) plane does not exceed 22 degrees of arc. At the end of PF cycles, the phase front vanishes in the warmest sample corners. This process is schematically illustrated in figures 1(a) and (b) and by photographs of the phase front in the a_2 section (figures 1(d) and (e)). The β angle value is due to a small component along c of the thermal gradient $\vec{G}_e$ (figure 1(b)). In such a case (E_z smaller than 250 V cm^{-1}) the phase front during FP cycles is also quasi-planar and the β angle is similar in magnitude but with an opposite sign to the PF ones (figure 1(c)). Diffraction fringes of an He–Ne laser beam propagating along the c axis demonstrate the domain structure existence in the orthorhombic phase with both permissible orientations of the domain walls. As already shown the domain texture is more regular and the domain width greater during FP cycles than during PF ones. Furthermore only one permissible wall orientation is observed during FP cycles.

When the dc applied electric field E_z is equal to or greater than 300 V cm^{-1}, PF cycles appear similar to ones previously described (figure 2(a)). The creation of the orthorhombic phase corresponds to a polydomain state which is simplified step by step with decreasing temperature. During the stabilization of temperature 15 degrees below the transition temperature the crystal becomes almost monodomain. When the FP transition begins the crystal is wholly monodomain and no diffraction of the laser beam crossing the sample can be observed. The FP cycle phenomena are new and described by the schematic representation in figure 2 and photographs in figure 3. Firstly the tetragonal phase is created at the warmest corners of the monodomain ferroelectric sample as shown in figure 2(b). Then in a very short time, less than a second, heterophase blocks appear all along the a_1 sample face (see figures 2(c) and 3(a)). The limit between this heterophase region and the monodomain ferroelectric one is an a_1 tetragonal plane. In the heterophase region paraelectric and ferroelectric stripes perpendicular to the c ferroelectric axis alternate in the sample. The observed diffraction of

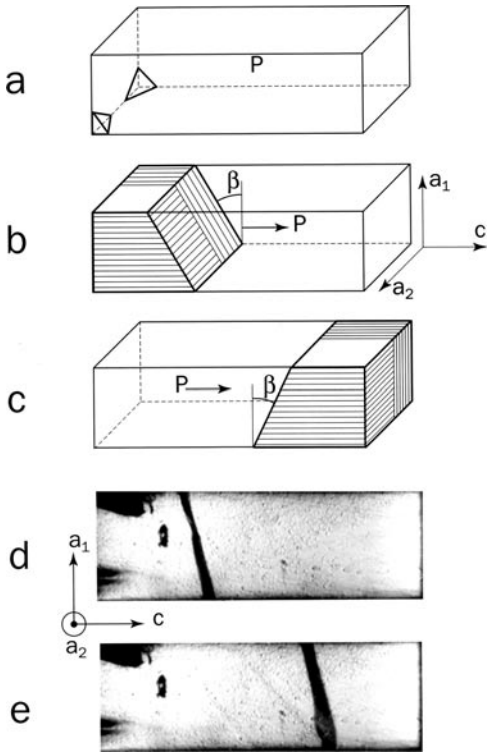

Figure 1. Phase coexistence in a crystal where E_z is lower in magnitude than 250 V cm^{-1}. PF cycle: schematic representation of the phase front and domain texture (a), (b) and photographs of the phase front in the a_2 section (d), (e). FP cycle: schematic representation (c).

the laser beam gives evidence for the existence of a domain structure inside the ferroelectric parts of the heterophase region. The phase fronts between ferroelectric and paraelectric stripes are almost in (001) planes (β less than 3 degrees of arc). The boundary between the heterophase region and the monodomain ferroelectric one starts out very quickly from the a_1 sample face in the a_1 direction. Its motion velocity gradually decreases with simultaneous enlargement of the stripe width (figures 3(a) and (b)). In figure 3(b), where the multilayer system is already simplified, the motion velocity is equal to 1 mm min^{-1}. After this dynamic process, it is possible to observe a quasistabilized phase front when it becomes similar to the zigzag phase front (Bornarel and Cach 1999) with cut down tips by the monodomain region (see in figures 2(d) and 3(d)). In this phase front a high dagger often alternates with a low one and the shape is easily distorted by growth defects as in figure 3(e) (Bornarel and Cach 1993, Kvitek and Bornarel 1997). When the boundary between the heterophase region and the monodomain ferroelectric one disappears (figure 3(f)), individual daggers on the coldest a_1 sample face remain inside the sample and finally vanish. These daggers are always polydomain.

3.2. Dielectric properties and thermal hysteresis

Results on dielectric constant ε_c' and loss constant ε_c'' versus temperature T and dc applied electric field E_z during PF and FP cycles are given in figure 4. The temperatures of appearance and disappearance of the phase front are indicated on the curves by arrows. As well known in KDP family crystals (Bornarel 1984), the ε_c' values at a given temperature are greater during a

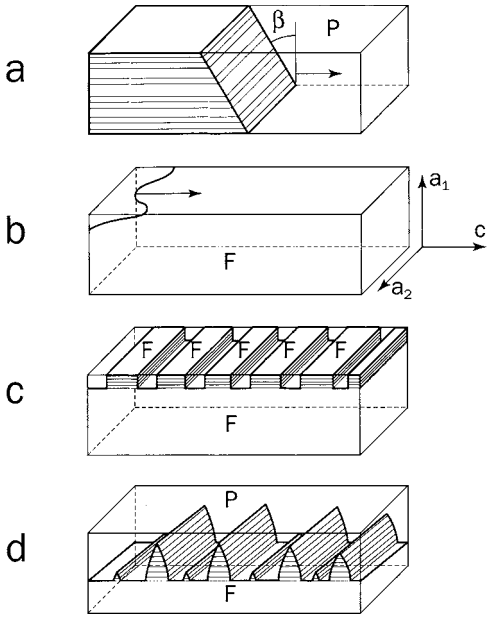

Figure 2. Phase coexistence in a crystal when E_z is equal in magnitude to 300–400 V cm^{-1}. Schematic representation of the phase fronts and domains during a PF cycle (a) and an FP one (b)–(d).

cooling cycle related to a heating one. Let us note the abrupt modification in the $\varepsilon'_c(T)$ curve ($E_z = 400$ V cm^{-1}) corresponding to the PF cycle (figure 4(c)).This is due to a jump in phase front motion and illustrates the temperature homogeneity inside the sample. In the present paper where a dc field E_z is applied, the most interesting phenomena is the thermal hysteresis variation. When E_z is smaller than 250 V cm^{-1}, the thermal hysteresis measured with the lower platinum resistor is equal to around 5×10^{-2} K. It has been previously demonstrated that the temperature of the crystal remains constant during the phase coexistence when $E_z = 0$. This is illustrated in figure 4(a) where the appearance of the phase front occurs at the sample temperature 208.65 K during the PF cycle and the FP one (see the arrows on the curves). The thermal hysteresis measured on the platinum resistor when E_z is smaller than 250 V cm^{-1} cannot be explained only by the temperature difference between the resistors of the upper and the lower a_1 sample faces (about 2×10^{-2} K), but this thermal hysteresis never exceeds 6×10^{-2} K with an uncertainty of a few 10^{-2} K. In contrast, the thermal hysteresis value jumps to 0.3 K as shown in figure 5 when E_z is greater than 250 V cm^{-1}, i.e. when the FP transition shows the phenomena described in figures 2 and 3. The purpose of the next section is to propose an explanation for this phase coexistence with heterophase stripes. It is also necessary to interpret the thermal hysteresis variation while the classical Landau–Devonshire theory predicts a decrease with E_z and not an abrupt increase.

4. Discussion

A complete study of the phase coexistence needs an analysis of the dynamic process taking into account the heat spreading in the sample during phase front motion. Unfortunately the available data are not sufficient. So firstly we analyse only the anisotropy of different energy

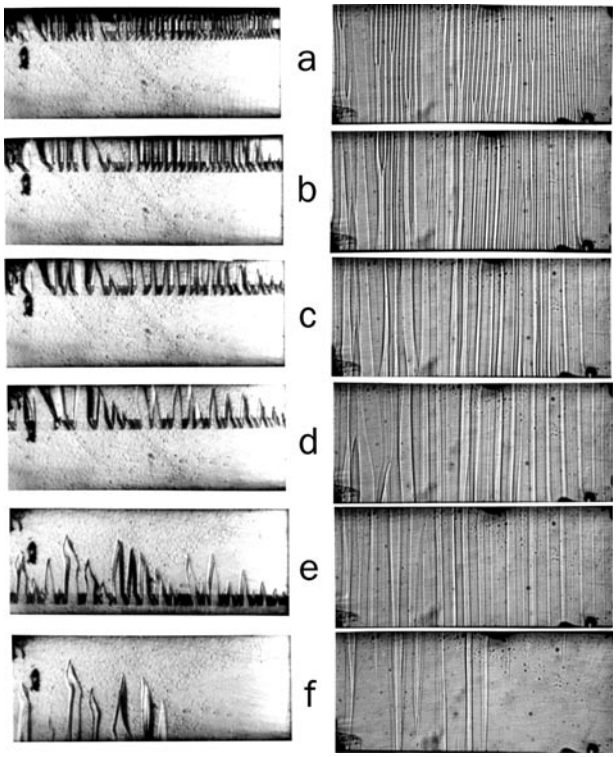

Figure 3. Phase coexistence in a DKDP crystal under $E_z = 400$ V cm^{-1} during an FP cycle: phase fronts in the a_2 section (left) and in the a_1 section (right).

contributions: electrostatic energy, chemical energy due to the thermal gradient existence and mechanical energy. After that, phenomena reported in the present paper are discussed.

The electrostatic energy is important when the E_z magnitude is sufficient to induce a monodomain orthorhombic region. If the crystal undergoes phase transition in these conditions, the phase front is observed as parallel to the c ferroelectric axis. Therefore the interface between both regions is non-charged (Bastie *et al* 1980, Bornarel 1991). In the case of small E_z values, a polydomain texture exists corresponding to smaller electrostatic energy. Then the long range influence of the monodomain state is reduced to the volume near the domain tips, i.e. near the parts of phase front non-parallel to the c axis (Bornarel and Cach 1999).

The chemical energy induced by the temperature gradient $\vec{G}_e$ forces the phase front to be in the isotherm surface corresponding to the transition temperature T_c when E_z is equal to zero: the chemical energy at this temperature takes the same value in the ferroelectric phase and in the paraelectric one. In the present paper, $\vec{G}_e$ is approximately parallel to the a_1 axis. Then the optimal orientation of the phase front to minimize the chemical energy should be an a_1 plane (Bornarel *et al* 1996). Let us note that here the $\vec{G}_e$ value ($G_e \approx 10^{-3}$ K mm^{-1}) could induce a temperature difference between opposite sides of the sample lower than 10^{-2} K. This is far smaller than the maximum temperature range of phase coexistence calculated with the help of Landau–Devonshire theory (0.2 K). Then in the present case, chemical energy does not play an important role.

The anisotropy of the mechanical energy is demonstrated with the help of Khachaturyan's theory where we calculate the work of elastic forces caused by the inclusion of an orthorhombic

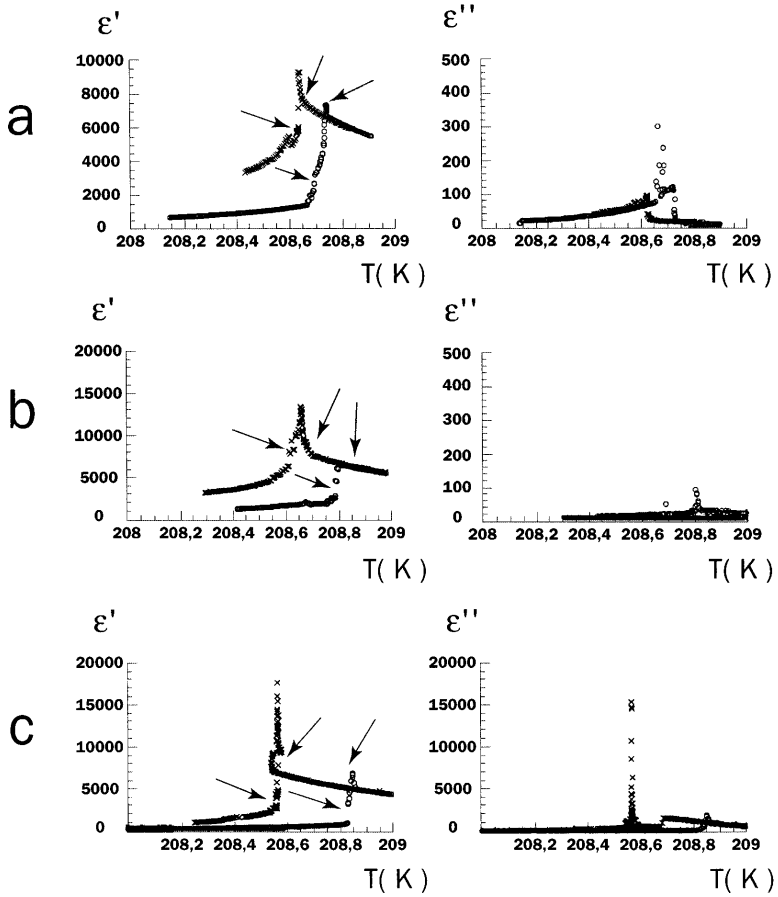

Figure 4. Dielectric constant ε_c' and loss constant ε_c'' versus temperature T during PF (x) and FP (○) cycles with crystal under different E_z values: (a) $E_z = 0$ V cm^{-1}; (b) 150 V cm^{-1}; (c) 400 V cm^{-1}.

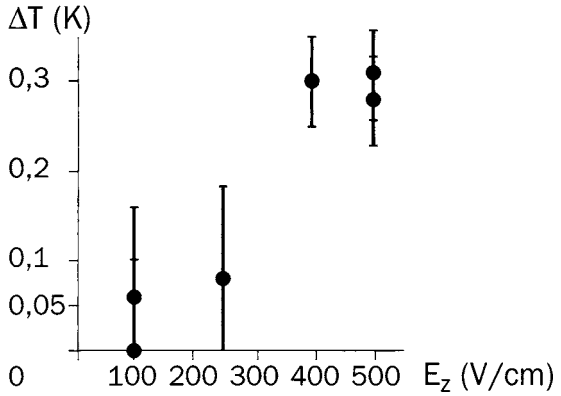

Figure 5. Thermal hysteresis in relation to the dc applied electric field E_z.

phase region inside an infinite crystal in the tetragonal phase. The inclusion is taken as an infinitesimally thin plate with homogeneous spontaneous strain $\tilde{u}$. The orientation of this plate

shaped inclusion is defined by its normal vector $\vec{n}$ and the energy density B can be written as follows:

$$B(\vec{n}) = \lambda_{ijkl} u_{ij} u_{kl} - n_i \sigma_{ij} \Omega_{jl} \sigma_{lm} n_m \tag{1}$$

with

$$\sigma_{ij} = \lambda_{ijkl} u_{kl}$$

$$\Omega^{-1}_{jl} = \lambda_{qjpl} n_p n_q$$

where λ_{ijkl} are the elastic constants and u_{ij} and σ_{ij} the mechanical strain and stress components, respectively.

Below, for elastic constants and strain components, usual notations for indices are used ($x = 1, y = 2, z = 3$). Previous works give λ_{ijkl} and u_{ij} values near the transition temperature:

$u_{11} = u_{22} = 1 \times 10^{-4}$ (Aleshko-Ozhevskij 1992)

$u_{33} = 6.5 \times 10^{-4}$ (Zeyen *et al* 1976)

$\lambda_{1111} = \lambda_{2222} = 7.2 \times 10^{10}$ N m^{-2} $\qquad$ $\lambda_{1122} = -1 \times 10^{10}$ N m^{-2}

$\lambda_{1313} = \lambda_{2323} = 1.2 \times 10^{10}$ N m^{-2} $\qquad$ $\lambda_{3333} = 5.4 \times 10^{10}$ N m^{-2}

$\lambda_{1133} = \lambda_{2233} = 1.2 \times 10^{10}$ N m^{-2} (Landolt–Börnstein 1981)

$\lambda^{P}_{1212} = 0.6 \times 10^{10}$ N m^{-2} (Litov and Uehling 1970)

$u_{12} = 7.2 \times 10^{-3}$ (Zeyen and Meister 1976) or 9.6×10^{3} N m^{-3} (Nelmes *et al* 1987).

An average macrostrain $\bar{u}$ can be defined when the domain structure exists in the orthorhombic phase. The $\bar{u}$ value depends on the ratio γ between the total volume of positive shear strained domains and the volume of the ferroelectric phase ($0 < \gamma < 1$). For example $\bar{u}_{12} = \pm u_{12}$ in monodomain cases ($\gamma = 0$ or 1) and is equal to zero in very regular polydomain ones ($\gamma = 1/2$). The energetical problem is described not only by the three terms mentioned above but also by crossing terms coupling temperature gradient $\vec{G}_e$, spontaneous strain tensor and polarization. For example, the piezoelectric coupling between shear strain component u_{12} and polarization is evident during the transition: whereas the elastic constant λ^{P}_{1212} for constant polarization P_z is almost constant (Litov and Uehling 1970), the elastic constant λ^{E}_{1212} for constant field E_z is influenced by the piezoelectric coupling. This is a function of the dielectric susceptibility which increases considerably as illustrated in figure 4. As a consequence the value $\lambda^{E}_{1212} = 0.6 \times 10^{10}$ N m^{-2} measured at temperatures far from the transition is reduced to the value $\lambda^{E}_{1212} = 0.1 \times 10^{10}$ N m^{-2} at the transition temperature. Then the λ^{E}_{1212} value changes abruptly near the transition and this must be taken into account in calculations. Let us now consider the two different experimental observations of the phase front shape and explain them with the help of the different previous energy contributions.

4.1. Quasi-planar phase front near (001) plane

When the phase front exhibits a quasi-planar shape with an angle β ($\leqslant 22^\circ$) related to the (001) plane, the ferroelectric phase is always clearly polydomain. When E_z is equal to zero, the dense domain structure is regular and $\bar{u}_{12} \cong 0$ ($\gamma = 1/2$). In such conditions, the electrostatic energy is negligible and the variation of the mechanical energy B calculated with the help of relation (1) (and with $u_{xx} = 1 \times 10^{-4}$, $u_{zz} = 6.5 \times 10^{-4}$, $\lambda_{1212} = 0.6 \times 10^{10}$ N m^{-2}) describes the experimental results: the potential profile $B(\beta)$ is minimum for β equal to zero (phase front perpendicular to c) as illustrated by curve a of figure 6. The existence of a small temperature gradient can tilt the phase front relative to the (001) plane as represented in figures 1(b) and (c). It clearly appears in figure 6 (curve a with B in a logarithmic scale) that the phase front tilt

out of the (001) plane becomes more and more difficult when β increases above 15°. Figure 6, curve a′ drawn with λ_{1212} equal to 0.1×10^{10} N m^{-2} corresponds to the softening process at the transition. The $B(\beta)$ curve does not change and the minimum value for B is still obtained at β equal to zero.

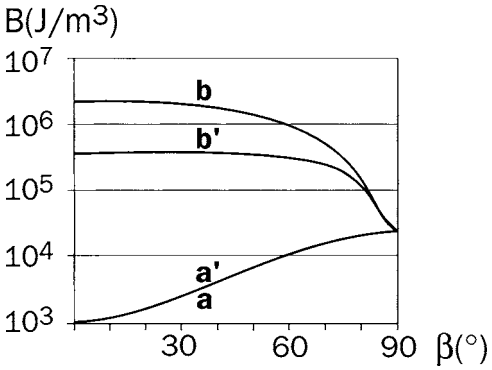

Figure 6. Energy density B plotted versus β angle: a, $\bar{u}_{xy} = 0$; b, $\bar{u}_{xy} = 9.6 \times 10^{-4}$ with $\lambda_{1212} = 0.6 \times 10^{10}$ N m^{-2}; a′ and b′ correspond to the same $\bar{u}_{xy}$ values as a and b respectively but with $\lambda_{1212} = 0.1 \times 10^{10}$ N m^{-2}.

4.2. PF and FP transitions with a small dc E_z field

The experimental results demonstrate that the phase front shape is completely different when the ferroelectric region is polydomain with a dense texture than when it is a monodomain one: as previously observed when a strong dc electric field E_z is applied (Bastie *et al* 1980, Bornarel 1991), the phase front between the ferroelectric monodomain region and the paraelectric one is in an a plane parallel to the c axis. The variation of $B(\beta)$ with $\bar{u}_{12} = u_{12}$ and $\lambda_{1212} = 6 \times 10^9$ N m^{-2} shown in figure 6(b) well illustrates this result: the minimum is obtained when β is equal to 90°. If the softening is taken into account ($\lambda_{1212} = 1 \times 10^9$ N m^{-2}) the $B(\beta)$ curve values are smaller as shown in figure 6, curve b′ but the minimum value is again obtained when β is equal to 90°. In this case the electrostatic energy becomes more important and is a minimum when β is equal to 90° but anisotropy of the mechanical density $B(\beta)$ also explains the experimental results.

What happens when a small dc applied electric field E_z is applied? If the domain texture remains dense and if the crystal polarity is not zero, the $B(\beta)$ variation can be calculated using a $\bar{u}_{12}$ value different from zero (in the following $\lambda_{1212} = 6 \times 10^9$ N m^{-2} is used but this choice does not change qualitatively the demonstration). Figure 7 gives the variation $B(\beta)$ with $\bar{u}_{12}$ as parameter. When $\bar{u}_{12}$ remains smaller than a critical value (0.1026 $\bar{u}_{12}$ without softening and 0.25 $\bar{u}_{12}$ with softening as shown in figure 8) the minimum of the $B(\beta)$ curve happens when β is equal to zero; if $\bar{u}_{12}$ becomes greater than this value, the $B(\beta)$ minimum happens when β is equal to 90°. Then during the PF cycles with E_z equal to 300 V cm^{-1} (or 400 V cm^{-1}), the ferroelectric region is still polydomain with a very small $\bar{u}_{12}$ and the phase front is a quasiplanar one approximately perpendicular to the c axis (figure 2(a)). In contrast, during the FP cycles with the same applied electric field E_z values, the sample is almost monodomain and $\bar{u}_{12}$ not far from u_{12}. Then the orientation of the phase front parallel to c ($\beta = 90°$) is more favourable. But two remarks allow us to understand the phase coexistence shown in figure 3. Firstly the B minimum value at $\beta = 90°$ (figure 6(b) or 7) is equal to 2.45×10^4 J m^{-3}, which is greater than the minimum value obtained with the polydomain region at $\beta = 0$ (figures 6(a) and 7):

1.13×10^3 J m^{-3}. So the direct transition from monodomain ferroelectric phase to tetragonal phase may be facilitated if intermediate polydomain regions can be created. The second remark concerns the character of the creation of a new phase which is a dynamic process with local heat exchange between the two phases. These two remarks are only arguments to understand the figure 3 process. Our purpose is not to model the dynamic of the process but only the obtained phase front shape: the creation on the warmest a_1 face of the heterophase stripes improves the local heat exchange between the two phases, decreases the phase front surface parallel to c ($B(90^\circ) = 2.45 \times 10^4$ J m^{-3}) and creates phase front parts perpendicular to c with $B = 1.13 \times 10^3$ J m^{-3}. Let us suppose, to model the situation, that the heterophase region can be described from the point of view of macrostrains as a special phase. In comparison with the monodomain ferroelectric phase, this special region exhibits only a component of macrostrain $\bar{u}_{zz} = (1 - \omega)u_{zz}$, $\bar{u}_{xx} = (1 - \omega)u_{xx}$, $\bar{u}_{xy} = (1 - \omega)u_{xy}$ if ω is the ratio between the new tetragonal phase volume and the total volume of the heterophase region ($\bar{u}_{12} = 0$ in paraelectric stripes but also in the ferroelectric ones because these are polydomain). It is possible to estimate the mechanical energy due to the boundary between the heterophase inclusion (with $\bar{u}_{zz}$, $\bar{u}_{xx}$ and $\bar{u}_{xy}$ given above) and the infinite ferroelectric monodomain phase (with $\bar{u}_{zz}$, $\bar{u}_{xx}$ and $\bar{u}_{xy}$ as strains). The situation is similar to the ones in figure 6, curve b (or b′) corresponding to an inclusion of a monodomain ferroelectric phase in the tetragonal phase. The strain components are now $u_{xy} - 0 = \bar{u}_{xy}$, $u_{zz} - \bar{u}_{zz} = \omega u_{zz}$ and $u_{xx} - \bar{u}_{xx} = \omega u_{xx}$. The minimum B value is obtained when β is equal to 90° as experimentally observed (boundary parallel to the c axis). Its value can be calculated because the relation (1) is bilinear versus u_{xx} and u_{zz} and it is easy to show that the B^* value corresponding to the heterophase region–monodomain phase boundary is

$$B^*(90^\circ) = B(90^\circ)\omega^2.$$

If the ω value is taken as observed in figure 3 around 1/3 (and $B(90^\circ) = 2.45 \times 10^4$ J m^{-3}), $B^*(90^\circ)$ is equal to 2.7×10^3 J m^{-3}. The contribution of the phase front parts perpendicular to c inside the heterophase region is negligible at the beginning of the process but increases with the motion of the boundary inside the crystal. In conclusion, the Khachaturyan model of inclusion allows a satisfactory model for the observed phenomena in figures 1–3.

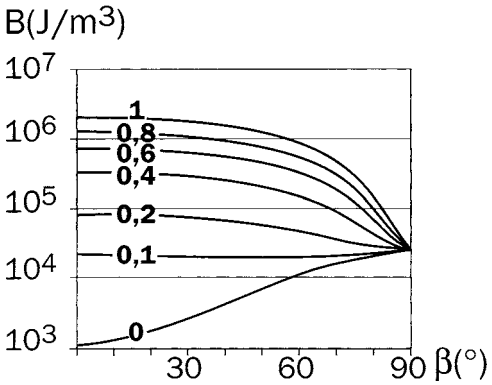

Figure 7. Mechanical energy density B plotted versus β angle with $\bar{u}_{12}$ as parameter (with $\lambda_{1212} = 6 \times 10^9$ N m^{-2}). On the curves is indicated n (with $\bar{u}_{12} = nu_{12}$).

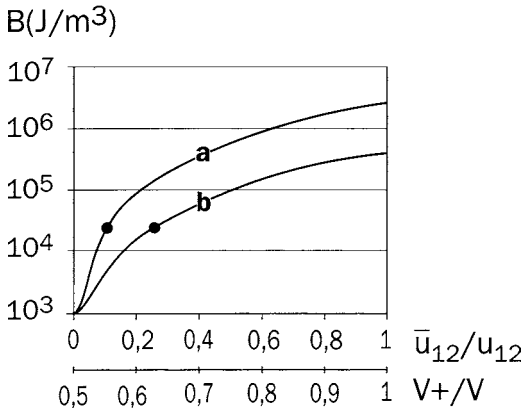

Figure 8. Energy density B for β equal to zero plotted versus $\bar{u}_{12}$ without (a) and with (b) softening (the ratio $V+/V$ between the volume of the domains + and the total volume of the ferroelectric region is also indicated). The black points indicate $B(0^\circ)$ values equal to $B(90^\circ)$ ones.

4.3. Thermal hysteresis of the transition

Now the strong modification in the thermal hysteresis at the transition illustrated in figures 4 and 5 is understandable. When the dc applied electric field E_z is smaller than 250 V cm^{-1} the phase coexistence interval in T is only a function of the temperature rate and of the defects inside the sample as usual. When E_z is greater than 300 V cm^{-1}, the phase front appearance in a c face is energetically impossible ($B(\beta = 0^\circ)$ increases until 2.2×10^6 J m^{-3}). The best orientation for the phase front corresponds to an a_1 plane (with $B(\beta = 90^\circ) = 2.45 \times 10^4$ J m^{-3}, which is 20 times more than the previous situation with $B(\beta = 0^\circ) = 1.13 \times 10^3$ J m^{-3}). Furthermore, to facilitate the heat exchange and to decrease the needed energy, the heterophase phenomenon appears. The necessary free energy induces a jump ΔT in the temperature appearance of the paraelectric phase as shown in figure 5. It is possible to evaluate ΔT by calculation of the volumic free energy variation ΔF during the creation of the heterophase region which corresponds to a δ part of the total crystal volume. ω is, as previously, the ratio in the heterophase region between the tetragonal phase and the total volume of the heterophase region, P the polarization and S the entropy.

$$\Delta F = \delta \left(\frac{B\omega^2}{2} + S\,\Delta T(1-\omega) \right) + (1-\delta)(S\,\Delta T - PE) \tag{2}$$

and by minimization related to ω and δ are obtained the following relations:

$$\omega^* = \left[\frac{2PE}{B} \right]^{1/2} \qquad \Delta T = \frac{[2BPE]^{1/2}}{S} \tag{3}$$

for the ω value and for the thermal hysteresis at the beginning of the phenomenon corresponding to figure 3(a). The factor $\frac{1}{2}$ in the $B\omega^2/2$ term is due to the elastic relaxation (Khachaturyan 1983). Using the data $P = 4.2 \times 10^{-2}$ C m^{-2} (Strukov *et al* 1972) and $E = 3 \times 10^4$ V m^{-1} it is possible to obtain $\omega^* = 0.32$. The uncertainty of the S value is greater: 6.8×10^4 J K^{-1} m^{-3} (Strukov *et al* 1968), 3.3×10^4 J K^{-1} m^{-3} (Bantle 1942), 1.7×10^4 J K^{-1} m^{-3} (Smolenskii 1984) and also on the ΔT value: between 0.11 K and 0.46 K. These results are in good agreement with the experimental data if the uncertainties in all the used parameters are taken into account. In a more accurate study, the different contributions in free energy due to the chemical energy (small thermal gradient) the electrostatic energy and their correlations with

the mechanical energy must be taken into account. The interesting feature is that the results for ω^* and ΔT are already in correct agreement which proves the great importance of the mechanical energy due to the interphase.

5. Conclusion

The phase coexistence between the ferroelectric–ferroelastic phase and the paraelectric–paraelastic one in DKDP crystals has been studied with application of small dc applied electric field E_z. These experimental studies confirm for very small E_z values, in PF as in FP cycles, the results already published without field: the phase front is quasiplanar, shaped approximately perpendicularly to the c ferroelectric axis, and the ferroelectric phase is polydomain. When the E_z value becomes greater than a critical value ($\approx$300 V cm^{-1}), a special phenomenon appears during FP cycles with a heterophase region with alternate stripes of ferroelectric polydomain phase and paraelectric phase. The other part of the crystal is in a ferroelectric monodomain phase. It has been demonstrated that the mechanical energy due to the interphase is the most important contribution. Using the Khachaturyan results, all the observed phase front shapes and phenomena have been explained as well as the jump in the transition thermal hysteresis. These results correspond to DKDP crystals but can be used more generally. Firstly the model could be used in other transitions such as structural transitions, ferroelastic transitions and ferroelectric–ferroelastic transitions where the interphase energy plays a great role and where the presence of domains may change the situation (α–β transition of quartz for example).

The thermal hysteresis at the transition in different ferroelastics, as in the presented DKDP case, does not follow the prediction of the Landau theory: a small dc electric field or mechanical stress application induces an increase of the thermal hysteresis (which decreases obviously with strong fields). The theory could be directly applied only for a transition of first order which exhibits an important jump of the order parameter, and under small applied external fields (mechanical or electrical). Many examples can be found in the literature as in $KMnF_3$ (Stokka *et al* 1981, Stokka and Fossheim 1982) or in $SrTiO_3$ (Chrosh and Salje 1998, Gallardo *et al* 1996). It would be interesting to apply the calculation proposed here to these crystals with different permissible walls and possible interphase.

References

Aleshko-Ozhevskij O P 1992 *Sov. Phys.–Solid State* **34** 934
Bantle W 1942 *Helv. Phys. Acta* **15** 373
Bastie P, Bornarel J, Dolino G and Vallade M 1980 *Ferroelectrics* **26** 789
Bornarel J 1984 *Ferroelectrics* **54** 585
——1991 *Phase Transitions* **34** 147
Bornarel J and Cach R 1991 *Ferroelectrics* **124** 345
——1993 *J. Phys.: Condens. Matter* **5** 2977
——1999 *Phys. Rev.* **60** 3806
Bornarel J, Cach R and Kvitek Z 1996 *J. Phys.: Condens. Matter* **8** 7365
Bornarel J and Lajzerowicz J 1968 *J. Appl. Phys.* **39** 4339
Chabin M and Gilletta F 1977 *Ferroelectrics* **15** 149
Chrosh J and Salje E K H 1998 *J. Phys.: Condens. Matter* **10** 2817
Fousek J and Janovec V 1969 *J. Appl. Phys.* **40** 135
Gallardo M C, Jimenez J, del Cerro J and Salje E K H 1996 *J. Phys.: Condens. Matter* **8** 85
Hill R M and Ichiki S K 1964 *Phys. Rev.* **135** 1640
Khachaturyan A G 1983 *Theory of Structural Transformation in Solids* (New York: Wiley–Interscience)
Kvitek Z 1997 *J. Phys.: Condens. Matter* **9** 127
Kvitek Z and Bornarel J 1997 *Ferroelectrics* **190** 31
Landolt–Börnstein New Series 1981 *Ferroelectrics III* (Berlin: Springer)

Litov E and Uehling E A 1970 *Phys. Rev.* B **1** 3713
Nelmes R J, Tun Z and Kuhs W F 1987 *Ferroelectrics* **71** 125
Reese W 1969 *Phys. Rev.* **181** 905
Reese W and May L F 1968 *Phys. Rev.* **167** 504
Sidnenko E V and Gladkii W 1973 *Sov. Phys.–Crystallogr.* **17** 861
Smolenskii G A 1984 *Ferroelectrics and Related Materials* vol 3 (London: Gordon and Breach)
Stokka S and Fossheim K 1982 *J. Phys. C: Solid State Phys.* **15** 1161
Stokka S, Fossheim K and Samulionis V 1981 *Phys. Rev. Lett.* **47** 1740
Strukov B A, Amin M and Kopchik V A 1968 *Phys. Status Solidi* **27** 741
Strukov B A, Baddur A and Velichko J A 1972 *Sov. Phys.–Solid State* **13** 2085
Zeyen C M E and Meister H 1976 *Ferroelectrics* **14** 731
Zeyen C M E, Meister H and Kley W 1976 *Solid State Commun.* **18** 621